Differential effect of canagliflozin, a sodium-glucose cotransporter 2 (SGLT2) inhibitor, on slow and fast skeletal muscles from nondiabetic mice

大塚, 裕子

Biochemical Journal (2022) **479** 425–444
https://doi.org/10.1042/BCJ20210700

PORTLAND PRESS

Research Article

Differential effect of canagliflozin, a sodium–glucose cotransporter 2 (SGLT2) inhibitor, on slow and fast skeletal muscles from nondiabetic mice

Hiroko Otsuka[1], Hisashi Yokomizo[1], Shintaro Nakamura[1], Yoshihiro Izumi[2], Masatomo Takahashi[2], Sachiko Obara[2], Motonao Nakao[2], Yosuke Ikeda[1], Naoichi Sato[1], Ryuichi Sakamoto[1], Yasutaka Miyachi[1], Takashi Miyazawa[1], Takeshi Bamba[2,3] and Yoshihiro Ogawa[1,3]

[1]Department of Medicine and Bioregulatory Science, Graduate School of Medical Sciences, Kyushu University, Fukuoka, Japan; [2]Division of Metabolomics, Medical Institute of Bioregulation, Kyushu University, Fukuoka, Japan; [3]AMED-CREST, Tokyo, Japan

Correspondence: Hisashi Yokomizo (yokomizo.hisashi.727@m.kyushu-u.ac.jp) or Yoshihiro Ogawa (ogawa.yoshihiro.828@m.kyushu-u.ac.jp)

There has been a concern that sodium–glucose cotransporter 2 (SGLT2) inhibitors could reduce skeletal muscle mass and function. Here, we examine the effect of canagliflozin (CANA), an SGLT2 inhibitor, on slow and fast muscles from nondiabetic C57BL/6J mice. In this study, mice were fed with or without CANA under *ad libitum* feeding, and then evaluated for metabolic valuables as well as slow and fast muscle mass and function. We also examined the effect of CANA on gene expressions and metabolites in slow and fast muscles. During SGLT2 inhibition, fast muscle function is increased, as accompanied by increased food intake, whereas slow muscle function is unaffected, although slow and fast muscle mass is maintained. When the amount of food in CANA-treated mice is adjusted to that in vehicle-treated mice, fast muscle mass and function are reduced, but slow muscle was unaffected during SGLT2 inhibition. In metabolome analysis, glycolytic metabolites and ATP are increased in fast muscle, whereas glycolytic metabolites are reduced but ATP is maintained in slow muscle during SGLT2 inhibition. Amino acids and free fatty acids are increased in slow muscle, but unchanged in fast muscle during SGLT2 inhibition. The metabolic effects on slow and fast muscles are exaggerated when food intake is restricted. This study demonstrates the differential effects of an SGLT2 inhibitor on slow and fast muscles independent of impaired glucose metabolism, thereby providing new insights into how they should be used in patients with diabetes, who are at a high risk of sarcopenia.

Introduction

The skeletal muscle is a major metabolic organ regulating glucose homeostasis through insulin-stimulated glucose uptake and disposal [1,2]. It is composed of four major fiber types based on their contractile properties in adult mammals; a slow-twitch fiber expressing myosin heavy chain (MyHC) I and three fast-twitch fibers expressing MyHC IIa, IIx, and IIb [3]. For example, soleus (SOL), generally classified as slow skeletal muscle (slow muscle), has a high proportion of MyHC I and IIa fibers, whereas extensor digitorum longus (EDL), classified as fast skeletal muscle (fast muscle), has a high proportion of MyHC IIb fibers.

Slow-twitch fibers display a two- to three-fold higher mitochondrial density relative to fast-twitch fibers and are rich in myoglobin and oxidative enzymes, efficient in energy production by fatty acid oxidation, and thus suitable for sustained activities [4], whereas fast-twitch fibers are characterized by glycolytic metabolism and specialized for phasic activities [3,5,6]. Studies with rodents showed that insulin-mediated glucose uptake is higher in slow-twitch oxidative fibers than in fast-twitch glycolytic

Received: 26 September 2021
Revised: 19 January 2022
Accepted: 19 January 2022

Accepted Manuscript online: 20 January 2022
Version of Record published: 11 February 2022

Biochemical Journal (2022) 479 425–444
https://doi.org/10.1042/BCJ20210700

fibers [7,8]. There is considerable evidence that the proportion of slow-twitch oxidative fibers is decreased in disuse-induced skeletal muscle atrophy, obesity, and diabetes [8–11]. On the other hand, the proportion of fast-twitch glycolytic fibers is known to be decreased by aging and sarcopenia [12]. To date, how slow and fast muscles are differently regulated has not been fully understood [13].

Sodium–glucose cotransporter 2 (SGLT2) inhibitors are an oral antidiabetic drug that promotes urinary excretion of glucose in the renal proximal tubules. The negative energy balance during SGLT2 inhibition leads to the reduction of body weight (BW) and fat mass [14,15]. Given the complex and elaborate organ network originating from the kidney, it is interesting to speculate that SGLT2 inhibitors affect a variety of metabolic pathways in remote organs, outside the kidney. For instance, we have reported that SGLT2 inhibitors; ipragliflozin and canagliflozin (CANA), improve hepatic steatosis in obese mice and delay the onset of nonalcoholic steatohepatitis (NASH)-associated hepatocellular carcinoma in a murine model of human NASH, in association with 'healthy expansion' of the adipose tissue [16,17]. On the other hand, there have been clinical and experimental reports on cardio-renal protective effects of SGLT2 inhibitors in rodent models of diabetes and in patients with diabetes [18,19].

There has been a concern that SGLT2 inhibitors could induce skeletal muscle atrophy or sarcopenia [20,21]. As a catabolic response to carbohydrate/calorie loss, SGLT2 inhibitors may induce skeletal muscle degradation to increase the release of amino acids into the systemic circulation, which are transported to the liver as substrates for gluconeogenesis, thereby preventing hypoglycemia. Indeed, luseogliflozin has significantly decreased skeletal muscle index in patients with diabetes [21,22]. On the other hand, tofogliflozin or dapagliflozin has improved glycemic control and reduced BW without reducing muscle mass in patients with diabetes [14,20,23].

SGLT2 inhibitors were originally developed as antidiabetic drugs, and accumulating evidence has supported the use of SGLT2 inhibitors for the treatment of patients with either heart failure or chronic kidney disease, regardless of the presence or absence of diabetes, mainly based on the EMPEROR-reduced trial [24], DAPA-HF trial [25], and DAPA-CKD trial [26]. Based on these evidences, some SGLT2 inhibitors have been globally used for the treatment of nondiabetic patients with heart failure or chronic kidney disease. Additionally, besides diabetes, whether and how SGLT2 inhibition affects slow and fast skeletal muscles remains unclear, independent of impaired glucose metabolism. Therefore, nondiabetic model mice were used in this study to investigate the effect of CANA on the muscle mass and function.

Results

Ad libitum feeding experiments (2 weeks)

Increased grip strength in CANA-treated mice

There was no significant difference in BW and random blood glucose (BG) between CANA- and vehicle-treated mice at 2 weeks after the treatment (Figure 1A,B). Food intake was significantly increased in CANA-treated mice relative to vehicle-treated mice ($P < 0.01$) (Figure 1C). There were no significant differences in serum insulin concentration between the two groups (Figure 1D). Blood β-hydroxybutyric acid (β-OHB) was significantly increased in CANA-treated mice (Figure 1E). We found no significant change in slow and fast muscle weight in CANA-treated mice (Figure 1F and Supplementary Figure S1A). There was also no significant difference in liver weight between CANA- and vehicle-treated mice (Supplementary Figure S1B). Epididymal white adipose tissue (eWAT) weight was significantly decreased in CANA-treated mice (Supplementary Figure S1C).

There was no significant difference between CANA- and vehicle-treated mice in terms of running distance, an aerobic and endurance exercise with which to evaluate slow muscle function (Figure 1G). In contrast, grip strength, with which to evaluate fast muscle function, was increased in CANA-treated mice, but no significant difference was observed between the groups ($P = 0.05$) (Figure 1H).

Gene expression and metabolome analysis of slow and fast muscles

We next examined gene expression in SOL and EDL as slow and fast muscles, respectively, from CANA-treated and vehicle-treated mice (Figure 2A,B). The mRNA expression of muscle atrophy-related genes such as forkhead box transcription factor O1 (*Foxo1*), *Atrogin1*, and *p62* was significantly increased in slow muscle, but unchanged in fast muscle, from CANA-treated mice. The mRNA expression of hexokinase 2 (*Hk2*), which catalyzes the first step in glycolysis by converting glucose into glucose-6-phosphate (G6P), phosphofructokinase, muscle (*Pfkm*), pyruvate kinase muscle isozyme 1 (*Pkm1*), and pyruvate dehydrogenase E1 subunit α 1 (*Pdha1*) were increased in slow muscle, but unchanged in fast muscle from CANA-treated mice. The mRNA

Biochemical Journal (2022) **479** 425–444
https://doi.org/10.1042/BCJ20210700

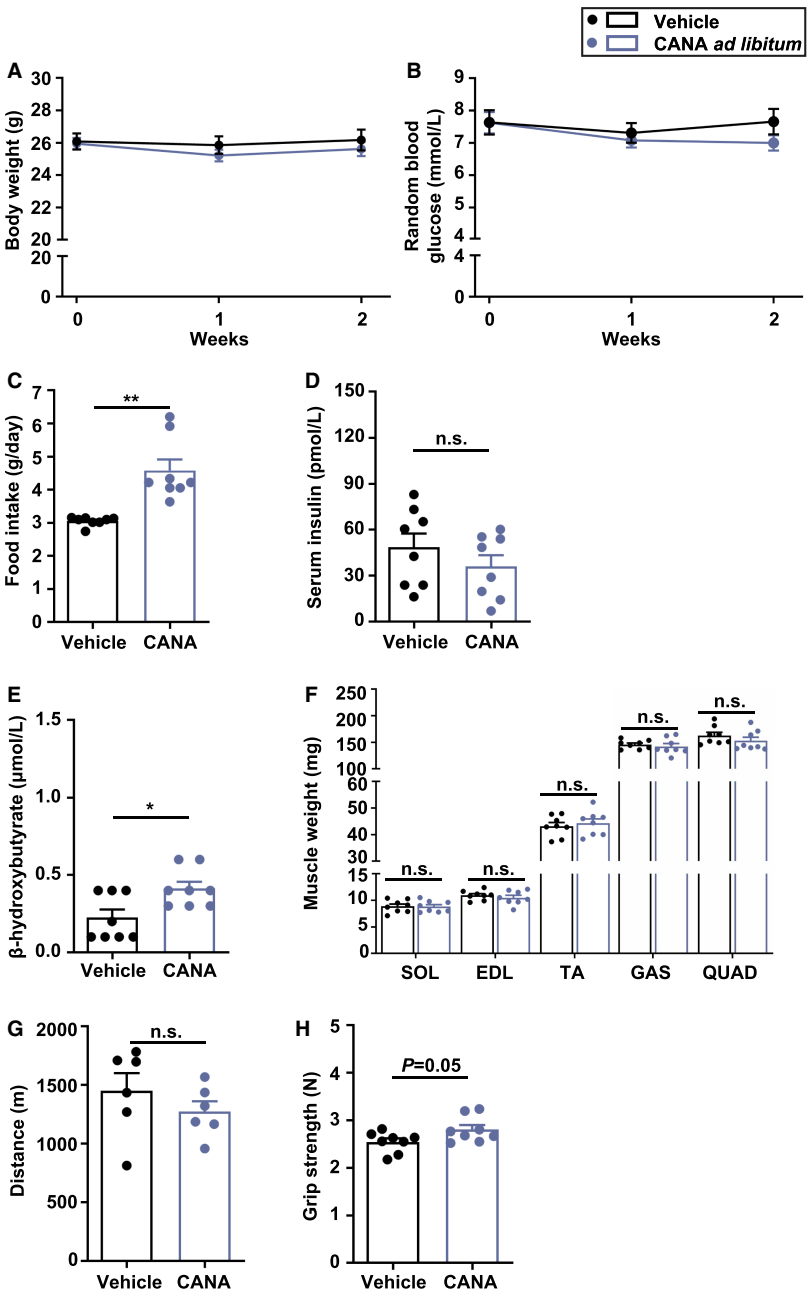

Figure 1. BW, BG, food intake, muscle weight, and function in slow and fast muscles from CANA-treated and vehicle-treated mice during the 2-week *ad libitum* feeding.

(**A**,**B**) Change in BW and random BG. (**C**) Food intake. (**D**) Serum insulin after 6-h fasting. (**E**) Blood β-OHB after 6-h fasting. (F) Right lower limb muscle weight. $n = 8$ mice/group. (G) Distance in treadmill exercise. $n = 6$ mice/group. (**H**) Grip strength. $n = 8$ mice/group. Data are expressed as the mean ± SEM. $^{*}P < 0.05$, $^{**}P < 0.01$, $^{***}P < 0.001$ vs. vehicle-treated mice (Student *t*-test). GAS: gastrocnemius; QUAD: quadriceps; TA: tibialis anterior.

expression of amino acid transporter and metabolism genes such as L-type amino acid transporter 2 (*Lat2*), alanine aminotransferase (*Alt1*, *Alt2*), and glutamine synthetase (*Gs*), β-oxidation-related genes such as acyl-CoA oxidase (*Aco*) and acetyl-CoA dehydrogenase, medium chain (*Mcad*), and lipolysis-related genes such as peroxisome proliferator-activated receptor α (*Ppara*), adipose triglyceride lipase (*Atgl*), and hormone-sensitive lipase (*Hsl*) was increased by CANA in slow muscle from CANA-treated mice.

PORTLAND PRESS

Biochemical Journal (2022) **479** 425–444
https://doi.org/10.1042/BCJ20210700

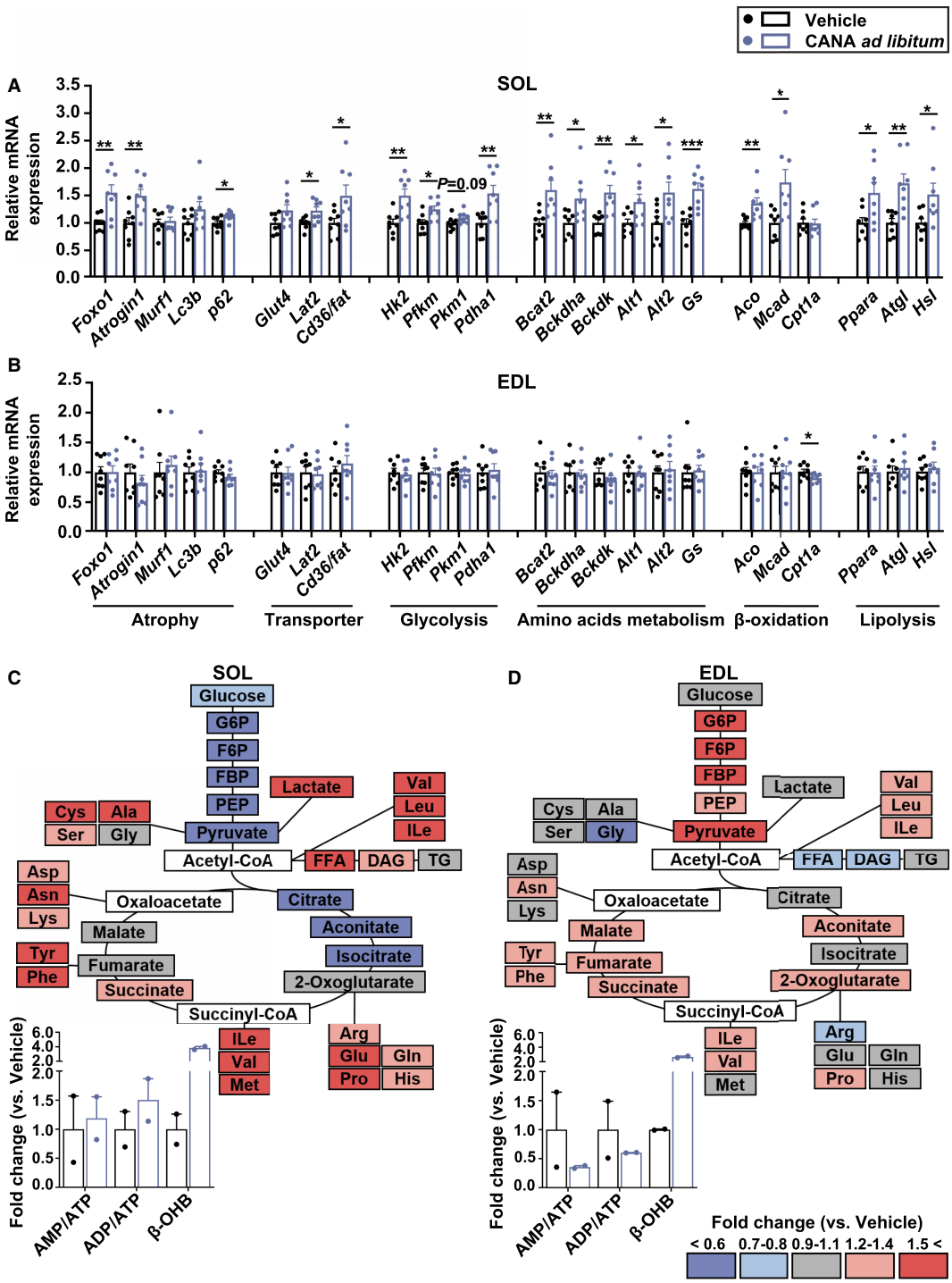

Figure 2. Gene expression and metabolites in slow and fast muscles from CANA-treated and vehicle-treated mice during the 2-week *ad libitum* feeding. Part 1 of 2

(**A**,**B**) The mRNA expression on SOL (**A**) and EDL (**B**). $n = 6$–8 mice/group. (**C**,**D**) The ratio of metabolites in CANA-treated mice to vehicle-treated mice in SOL (**C**) and EDL (**D**), calculated as fold change. Dark red indicates metabolites with the fold change ≧1.5 and dark blue indicates those with the fold change ≦ 0.6. Gray indicates those with no difference between CANA- and vehicle-treated mice. White indicates those undetected. Relative metabolite changes in ATP, ADP, AMP, and β-OHB were shown as bar graphs. White and blue bars represent vehicle- and CANA-treated mice, respectively. $n = 2$ mice/group. Data are expressed as the mean ± SEM. $^{*}P < 0.05$, $^{**}P < 0.01$, $^{***}P < 0.001$ vs. vehicle-treated mice (Student *t*-test). Ala: alanine;

Figure 2. Gene expression and metabolites in slow and fast muscles from CANA-treated and vehicle-treated mice during the 2-week *ad libitum* feeding. Part 2 of 2

Arg: arginine; Asn: asparagine; Asp: aspartic acid; BCAT2: branched chain amino acid transaminase 2; BCKDHa: branched chain keto acid dehydrogenase E1 subunit α; BCKDK: branched chain ketoacid dehydrogenase kinase; CD36/FAT: fatty acid translocase; CPT1a: carnitine palmitoyltransferase-1a; Cys: cysteine; Gln: glutamine; Glu: glutamic acid; Gly: glycine; His: histidine; Ile: isoleucine; Leu: leucine; Lys: lysine; Met: methionine; Phe: phenylalanine; Pro: proline; Ser: serine; Tyr: tyrosine; Val: valin.

We also examined the effect of CANA on metabolites in slow and fast muscles from two replicates (Figure 2C,D and Supplementary Tables S4 and S5). Overall, amino acids tended to be increased in slow muscle, with no change in fast muscle, from CANA-treated mice relative to vehicle-treated mice. On the other hand, glycolytic metabolites such as G6P, fructose 6-phosphate (F6P), fructose 1,6-bisphosphate (FBP), phosphoenolpyruvic acid (PEP), and pyruvic acid tended to be reduced in slow muscle, and tended to be increased in fast muscle from CANA-treated mice. In CANA-treated mice, free fatty acid (FFA) tended to be increased in slow muscle, but unchanged in fast muscle. Key metabolites in the TCA cycle were mostly unaffected in slow and fast muscles from CANA-treated mice. The ratios of AMP/ATP and ADP/ATP were unaffected in slow muscle, and reduced in fast muscle, from CANA-treated mice. β-OHB tended to be increased in slow and fast muscles, respectively, from CANA-treated mice.

Pair-feeding experiments (2 weeks)

Reduced grip strength in CANA-treated mice

Given that increased food intake could affect the metabolic phenotypes in CANA-treated mice, we adjusted the amount of food intake in CANA-treated mice to that in vehicle-treated mice. BW and random BG were significantly reduced in CANA-treated mice relative to vehicle-treated mice during the 2-week pair-feeding (Figure 3A–C). Serum insulin concentration was significantly decreased and blood β-OHB was significantly increased in CANA-treated mice relative to vehicle-treated mice ($P < 0.05$ and $P < 0.001$, respectively) (Figure 3D,E). Slow muscle weight was slightly reduced, but fast muscle weight was significantly reduced in CANA-treated mice ($P < 0.01$) (Figure 3F). However, there was no significant difference in slow and fast muscle weight per BW between CANA- and vehicle-treated mice (Supplementary Figure S2A). The liver and eWAT weight were significantly decreased in CANA-treated mice (Supplementary Figure S2B,C).

There was no difference in running distance between CANA- and vehicle-treated mice (Figure 3G). In contrast, grip strength was significantly reduced in CANA-treated mice relative to vehicle-treated mice ($P < 0.05$) (Figure 3H).

Gene expression and metabolome analysis of slow and fast muscles

The mRNA expression of muscle atrophy-related genes such as *Foxo1*, *Atrogin1*, and microtubule-associated protein 1 light chain 3 β (*Lc3b*) was significantly increased in both slow and fast muscles from CANA-treated mice relative to vehicle-treated mice (Figure 4A,B). The mRNA expression of *Glut4* and *Hk2* was unaffected in slow muscle, but increased in fast muscle from CANA-treated mice. The mRNA expression of *Alt2* and *Gs* was significantly increased in both slow and fast muscles. The mRNA expression of lipolysis-related genes such as *Ppara*, *Atgl*, and *Hsl* was increased in fast muscle from CANA-treated mice.

We next examined the effect of CANA treatment on metabolites in slow and fast muscles (Figure 4C,D and Supplementary Tables S6 and S7). Overall, some amino acids were significantly reduced in slow muscle, but unaffected in fast muscle from CANA-treated mice relative to vehicle-treated mice. Glycolytic metabolites were reduced in both slow and fast muscles from CANA-treated mice. FFA and metabolites in the TCA cycle were unaffected in both slow and fast muscles from CANA-treated mice. The ratios of AMP/ATP and ADP/ATP tended to be increased in fast muscle, but unaffected in slow muscle, from CANA-treated mice. β-OHB was significantly increased in slow and fast muscles, respectively, from CANA-treated mice.

Ad libitum feeding and pair-feeding experiments (4 weeks)

Metabolic phenotypes of CANA-treated mice

To investigate the long-term effect of CANA on slow and fast muscles, we extended the duration of CANA treatment up to 4 weeks. Mice were divided into three groups; those treated with vehicle and those with CANA

Biochemical Journal (2022) **479** 425–444
https://doi.org/10.1042/BCJ20210700

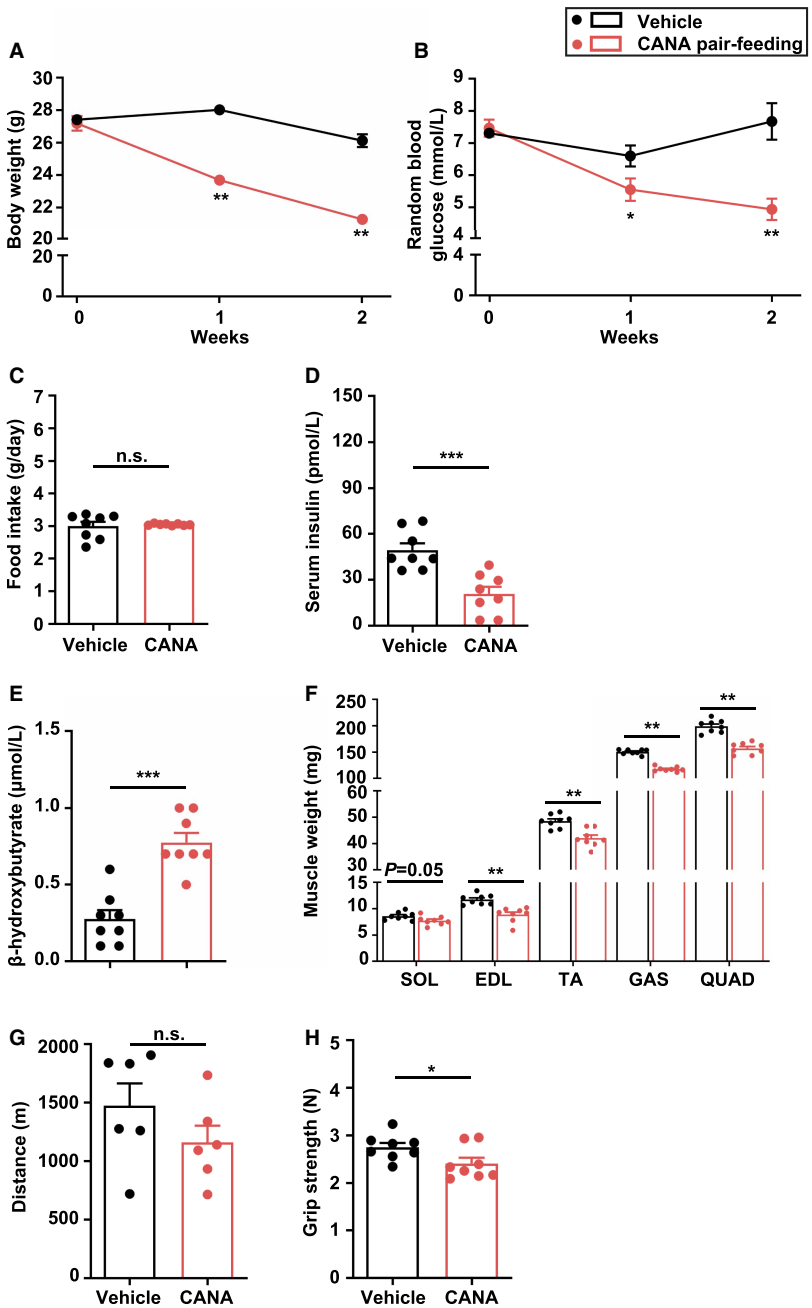

Figure 3. BW, BG, food intake, muscle weight, function in CANA-treated, and vehicle-treated mice during the 2-week pair-feeding.

(**A**,**B**) Change in BW and random BG. (**C**) Food intake. (**D**) Serum insulin after 6-h fasting. (**E**) Blood β-OHB after 6-h fasting. (**F**) Right lower limb muscle weight. $n = 8$ mice/group. (**G**) Distance in treadmill exercise. $n = 6$ mice/group. (**H**) Grip strength. $n = 8$ mice/group. Data are expressed as the mean ± SEM. $^{*}P < 0.05$, $^{**}P < 0.01$, $^{***}P < 0.001$ vs. vehicle-treated mice (Student *t*-test).

during the *ad libitum* feeding, and those treated with CANA during the 4-week pair-feeding. BW and random BG were unaffected in CANA-treated mice during the *ad libitum* feeding, but decreased during the pair-feeding, relative to vehicle-treated mice (Figure 5A,B). Food intake was significantly increased in CANA-treated mice relative to vehicle-treated mice, when fed *ad libitum* ($P < 0.01$) (Figure 5C). Fasting BG and insulin, and homeostasis model assessment of insulin resistance (HOMA-IR) at 16 h after fasting were not different

Biochemical Journal (2022) **479** 425–444
https://doi.org/10.1042/BCJ20210700

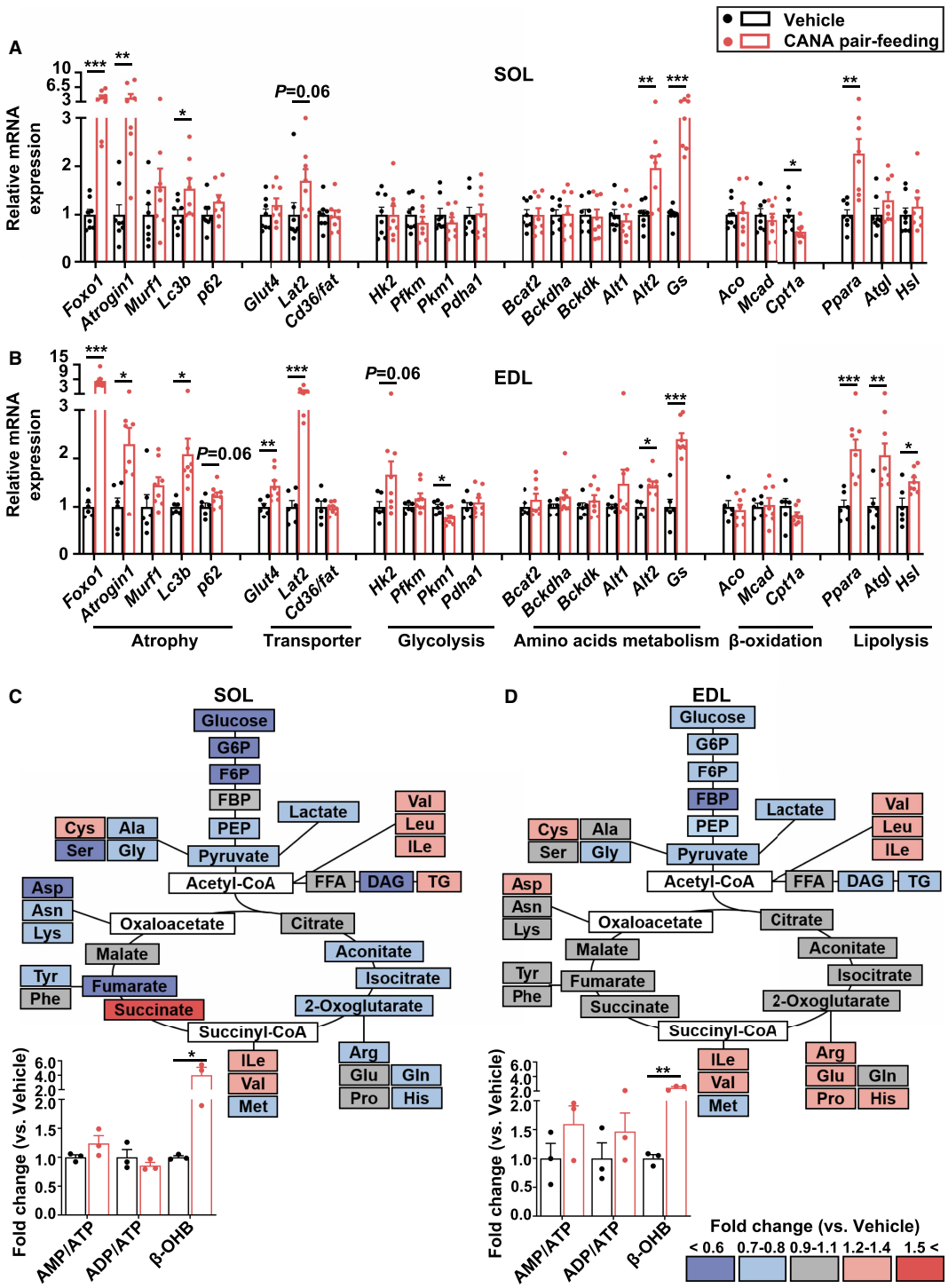

Figure 4. Gene expression and metabolites in slow and fast muscles from CANA-treated and vehicle-treated mice during the 2-week pair-feeding.

(**A**,**B**) The mRNA expression on SOL (**A**) and EDL (**B**). $n = 6$–8 mice/group. (**C**,**D**) The ratio of metabolites in CANA-treated mice to vehicle-treated mice in soleus (**C**) and EDL (**D**), calculated as fold change. The color of metabolites in the figure is shown as described above. $n = 3$ mice/group. Data are expressed as the mean ± SEM. $^{*}P < 0.05$, $^{**}P < 0.01$, $^{***}P < 0.001$ vs. vehicle-treated mice (Student *t*-test).

Biochemical Journal (2022) **479** 425–444
https://doi.org/10.1042/BCJ20210700

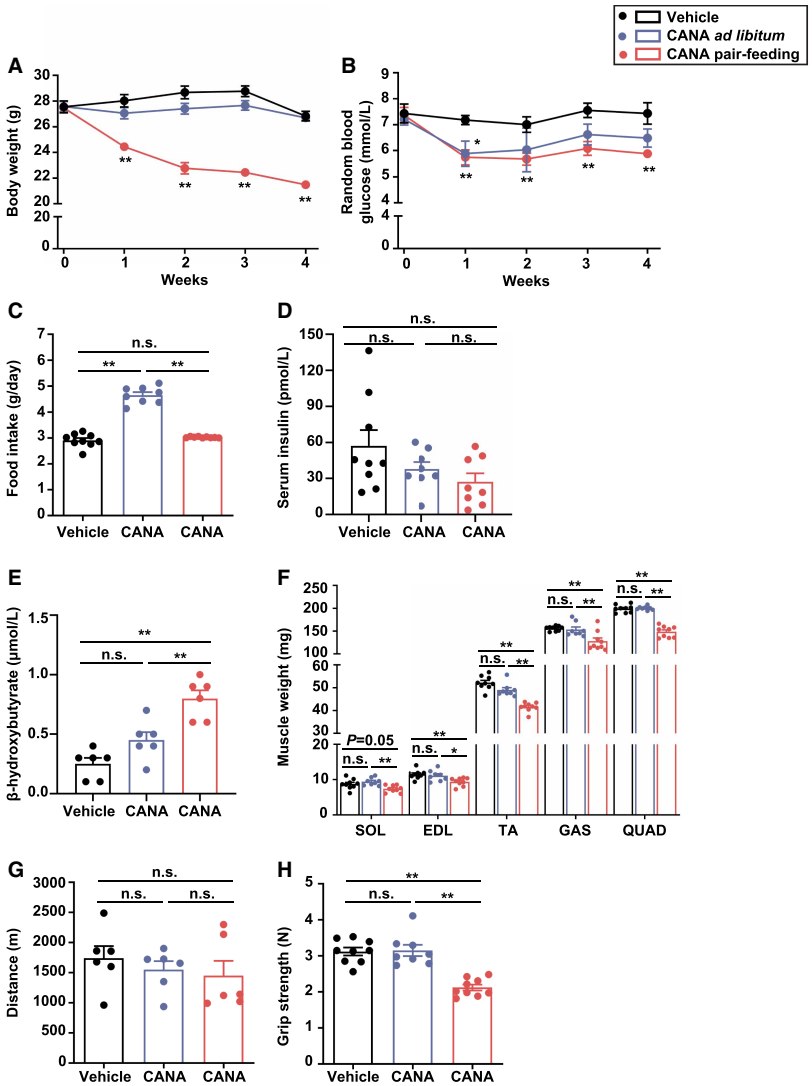

Figure 5. Effect of CANA on BW, BG, food intake, muscle weight, and function.

Mice were divided into three groups; those treated with vehicle and those with CANA during the 4-week *ad libitum* feeding, and those treated with CANA during the 4-week pair-feeding. (**A**,**B**) Change in BW and random BG. (**C**) Food intake. (**D**) Serum insulin after 6-h fasting. $n = 8$–9 mice/group. (**E**) Blood β-OHB after 6-h fasting. $n = 6$ mice/group. (**F**) Right lower limb muscle weight. $n = 8$–9 mice/group. (**G**) Distance in treadmill exercise. $n = 6$ mice/group. (**H**) Grip strength. $n = 8$–9 mice/group. White bars are shown for mice treated with vehicle, blue bars for those with CANA during the *ad libitum* feeding, and red bars for those treated with CANA during the pair-feeding. Data are expressed as the mean ± SEM, $^{*}P < 0.05$, $^{**}P < 0.01$, $^{***}P < 0.001$ vs. vehicle-treated mice (ANOVA).

between CANA-treated mice during the 4-week *ad libitum* feeding and during the 4-week pair-feeding, relative to vehicle-treated mice (Supplementary Figure S3A–C). There was no significant difference in serum insulin concentration among the three groups (Figure 5D). Blood β-OHB was increased in CANA-treated mice during the *ad libitum* feeding with no significant difference, and was significantly increased during the pair-feeding ($P < 0.01$) (Figure 5E). The slow muscle weight was maintained in CANA-treated mice during the *ad libitum* and pair-feeding. On the other hand, fast muscle weight was maintained in CANA-treated mice during the *ad libitum* feeding, but was significantly decreased during the pair-feeding ($P < 0.01$) (Figure 5F). There was no significant difference in slow and fast muscle weight per BW among the three groups (Supplementary Figure S4A). Liver and eWAT weight were maintained in CANA-treated mice during the *ad libitum* feeding,

but were significantly decreased during the pair-feeding (Supplementary Figure S4B,C). Running distance was unaffected among the three groups (Figure 5G). Grip strength was unaffected in CANA-treated mice during the *ad libitum* feeding, but significantly decreased in CANA-treated mice during the pair-feeding ($P < 0.01$) (Figure 5H).

The intensity of succinate dehydrogenase (SDH) staining was higher in slow muscle than in fast muscle from vehicle-treated mice. The intensity of SDH staining was unaffected in both slow and fast muscles from CANA-treated mice (Supplementary Figure S4D).

The effect of CANA on p-AMPK and p-mTOR expressions in slow and fast muscles

Since it is reported that CANA can increase p-AMPK expression in several cells [27], we performed western blotting and found that the expression of p-AMPK was slightly but not significantly increased in fast muscles from CANA-treated mice during the 4-week *ad libitum* feeding and 4-week pair-feeding relative to vehicle-treated mice, while not affected in slow muscles among the groups (Figure 6A,B and Supplementary Figure S5).

We also found that the expression of p-mTOR was significantly decreased in fast muscles from CANA-treated mice during the 4-week *ad libitum* feeding relative to vehicle-treated mice, and furthermore decreased in fast muscles from CANA-treated mice during the 4-week pair-feeding, while not affected in slow muscles among the groups (Figure 6A,B and Supplementary Figure S5).

DNA microarray analysis of slow and fast muscles

Given the marked phenotypic difference between CANA- and vehicle-treated mice during the pair-feeding, we performed microarray analysis of slow and fast muscles obtained from CANA- and vehicle-treated mice during the 4-week pair-feeding. Cluster analysis of gene expression pattern by the pvclust method using the normalized signal data revealed marked difference between slow and fast muscles. We also found marked difference in gene expression pattern in the skeletal muscles between CANA-treated and vehicle-treated mice (Supplementary Figure S6A); 650 and 816 genes were up-regulated in slow and fast muscles, respectively, and 555 and 400 genes were down-regulated in slow and fast muscles, respectively, from CANA-treated mice (Supplementary Figure S6B). Pathway analysis showed that genes related to PI3K–Akt signaling pathway are enriched in both slow and fast muscles from CANA-treated mice (Supplementary Figure S6C). Practically, the gene expression patterns in PI3K–Akt signaling pathways by cluster analysis were quite different between slow and fast muscles as well as vehicle- and CANA-treated mice (Supplementary Figure S7).

Gene expression and metabolome analysis of slow and fast muscles

The mRNA expression of muscle atrophy-related genes such as *Foxo1* and *Atrogin1* was increased in both slow and fast muscles from CANA-treated mice relative to vehicle-treated mice during the 4-week pair-feeding (Figure 7A,B). The mRNA expression of *Glut4* and glycolytic enzymes *Hk2* were unaffected in slow and fast muscles, whereas that of *Pfkm* and *Pkm1* was significantly reduced in fast muscle but not in slow muscle. The mRNA expression of *Lat2*, *Alt2*, and *Gs* as well as *Ppara* and *Atgl* was increased in both slow and fast muscles from CANA-treated mice. The mRNA expression of peroxisome proliferator-activated receptor γ co-activator 1α (*Pgc1a*), which is involved in the regulation of energy metabolism, mitochondrial biogenesis and increased slow-twitch fibers was significantly increased in slow muscle ($P < 0.01$), but unaffected in fast muscle from CANA-treated mice. Although the mRNA expression of *Pgc1a* was significantly increased in slow muscles from CANA-treated mice, muscle fiber type was unaffected in both slow and fast muscles from CANA-treated mice relative to vehicle-treated mice as determined by immunostaining of MyHC (Supplementary Figure S8).

We next examined the effect of CANA on metabolites in both slow and fast muscles (Figure 7C,D and Supplementary Tables S8 and S9). Overall, some amino acids were significantly reduced in slow muscle, but some amino acids tended to be increased in fast muscle, from CANA-treated mice relative to vehicle-treated mice. Glycolytic metabolites were reduced in slow muscle, but increased in fast muscle, from CANA-treated mice. FFA was reduced in slow muscle, but increased in fast muscle, from CANA-treated mice. Metabolites involved in the TCA cycle were unaffected in slow and fast muscles from CANA-treated mice. The ratios of AMP/ATP and ADP/ATP were unaffected in slow muscle, but significantly increased in fast muscle, from CANA-treated mice ($P < 0.01$). We also found that β-OHB was significantly increased in slow and fast muscles, respectively, from CANA-treated mice.

Biochemical Journal (2022) **479** 425–444
https://doi.org/10.1042/BCJ20210700

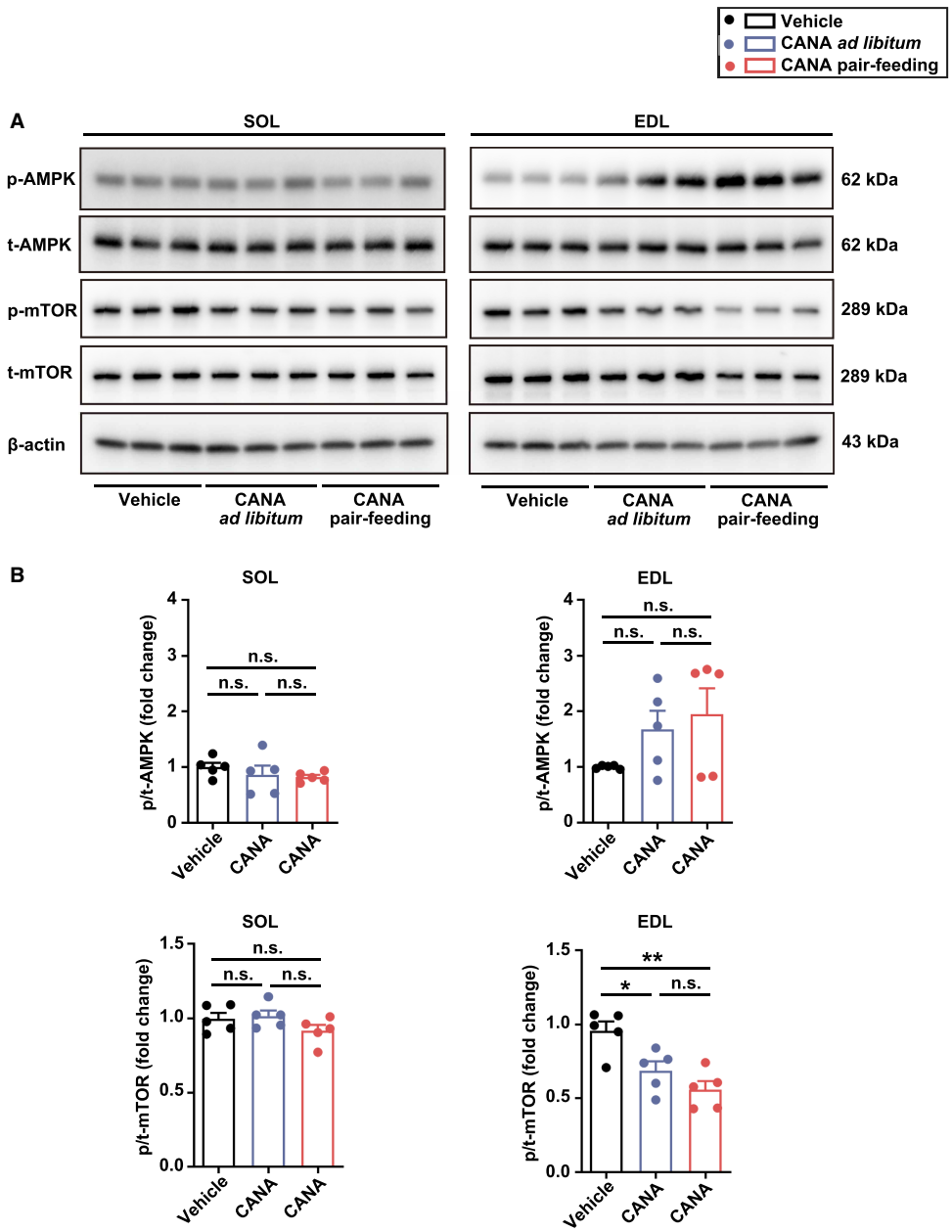

Figure 6. Effect of CANA on the phosphorylated p-AMPK and p-mTOR in SOL and EDL during the 4-week *ad libitum* or pair-feeding.

(**A**) Representative Western blots for the assessment of p-AMPK, t-AMPK, p-mTOR, and t-mTOR. (**B**) Quantitative bar graphs. $n = 5$ mice/group. Data are expressed as mean ± SEM. $^{*}P < 0.05$, $^{**}P < 0.01$ (ANOVA).

PI3K–Akt pathway activity in slow and fast muscles

We next examined the insulin-stimulated p-Akt levels in slow and fast muscles during the 4-week pair-feeding. Before insulin stimulation, there was no significant difference in p-Akt levels in both slow and fast muscles between CANA-treated and vehicle-treated mice (Supplementary Figure S9A–C). After insulin stimulation, p-Akt levels were increased by 4.3- and 3.2-fold in slow and fast muscles from vehicle-treated mice, respectively. On the other hand, p-Akt levels were increased by 10.9- and 6.5-fold in slow and fast muscles from pair-fed CANA-treated mice, respectively (Supplementary Figure S9A–C).

Biochemical Journal (2022) **479** 425–444
https://doi.org/10.1042/BCJ20210700

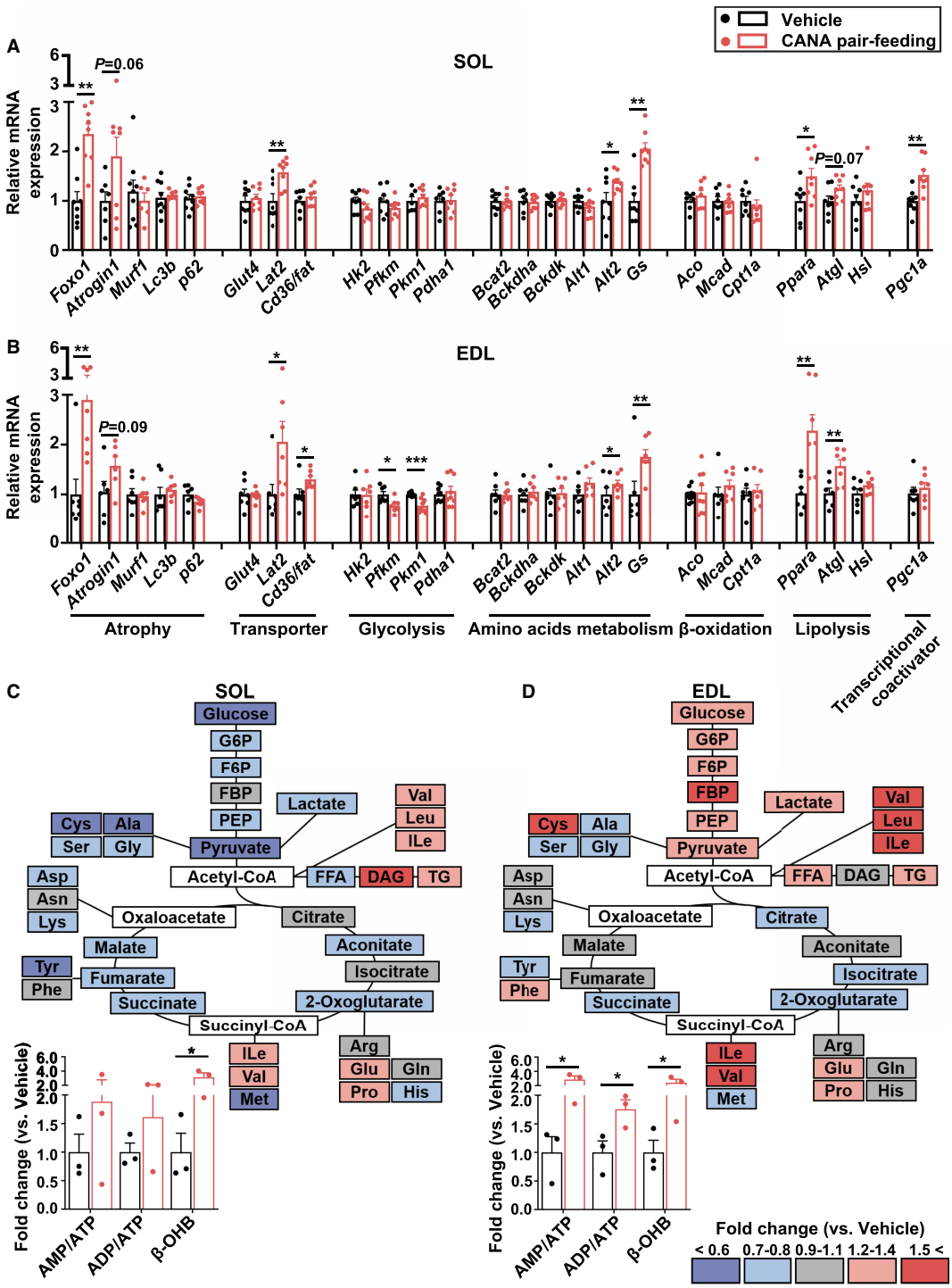

Figure 7. Effect of CANA on gene expression and metabolites in SOL and EDL during the 4-week pair-feeding.
(**A**,**B**) The mRNA expression on SOL (**A**) and EDL (**B**). $n = 6$–9 mice/group. (**C**,**D**) The ratio of metabolites in CANA-treated mice to those of vehicle-treated mice in SOL (**C**) and EDL (**D**), calculated as fold change. The colors of metabolites are shown as described above. $n = 3$ mice/group. Data are expressed as means ± SEM, $^{*}P < 0.05$, $^{**}P < 0.01$, $^{***}P < 0.001$ vs. vehicle-treated mice (Student *t*-test).

PORTLAND PRESS

Biochemical Journal (2022) **479** 425–444
https://doi.org/10.1042/BCJ20210700

Discussion

The skeletal muscle plays a critical role in the regulation of glucose homeostasis through insulin-stimulated glucose uptake and disposal. Because diabetes is often associated with loss of muscle mass and strength or sarcopenia, it is of great importance to understand how a particular antidiabetic drug could affect skeletal muscle mass and function [28,29]. Given that SGLT2 inhibitors induce catabolic responses by reducing glucose reabsorption in the renal proximal tubules [30], there has been a concern about their potential to induce skeletal muscle atrophy. However, the effect of SGLT2 inhibition on the skeletal muscle has not been fully understood [31], and if so, how slow and fast muscles are affected has not been addressed. This study was designed to elucidate the effect of an SGLT2 inhibitor, CANA on the skeletal muscle from nondiabetic mice.

In this study, CANA does not affect slow and fast muscle mass, when mice are fed *ad libitum*. Grip strength is increased, although running capacities are unaffected, suggesting the differential effect of SGLT2 inhibition on slow and fast muscles; fast muscle function appears to be affected preferentially over slow muscle function in mice, when fed *ad libitum*. Importantly, fast muscle mass and function are significantly decreased in CANA-treated mice during the pair-feeding, when slow muscle is unaffected. This is consistent with a previous report by Sano *et al.* [32] that grip strength is increased in patients with diabetes by ipragliflozin, which is accompanied by increased food intake. These observations, taken together, suggest that increased fast muscle function during SGLT2 inhibition is due at least in part to the compensatory increase in food intake.

The regulation of skeletal muscle mass depends upon the balance between protein synthesis and degradation [33–36]. We found that expression of muscle atrophy-related genes is slightly increased in parallel with increased amino acids in slow muscle from CANA-treated mice, when fed *ad libitum*. Since there is no appreciable reduction of slow muscle mass in CANA-treated mice, it is likely that increased amino acids, possibly as a result of increased food intake, are used as substrates for muscle protein synthesis in slow muscle, thus leading to the maintenance of slow muscle mass. The atrophic response is not induced, with no increased amino acids in fast muscle from CANA-treated mice, when fed *ad libitum*. However, during the pair-feeding, muscle atrophy-related genes are induced in both slow and fast muscles from CANA-treated mice. It is, therefore, conceivable that amino acids are used for muscle protein synthesis in CANA-treated mice even during the long-term food restriction, thus leading to the slight decrease in slow muscle mass (Supplementary Figure S10A). On the other hand, glycolytic metabolites are reduced in fast muscle as a result of selective loss of glucose during SGLT2 inhibition, when amino acids are increased by muscle proteolysis to be used as energy substrates, thus leading to significant reduction of fast muscle mass. Interestingly, during the long-term food restriction, glycolytic metabolites are increased with decreased expression of glycolytic genes in fast muscle, suggesting decreased glycolytic flux. Since fast muscle mass is reduced and amino acids are increased by muscle proteolysis, it is likely that amino acids may not be used sufficiently as energy substrates in response to decreased glycolytic flux (Supplementary Figure S10B). Taken together, the mass of both slow and fast muscles is maintained in CANA-treated mice, when fed *ad libitum*, through increased muscle protein synthesis via increased supply of amino acids, when muscle degradation might be slightly induced in catabolic response to SGLT2 inhibition. However, when food intake is restricted with reduced amino acid intake, protein degradation may exceed protein synthesis as a catabolic response to SGLT2 inhibition, which may cause loss of fast muscle predominantly over slow muscle. This discussion is consistent with the notion that muscle proteolysis occurs in fast muscle preferentially over slow muscle during starvation [37]. Previous studies have reported the effect of SGLT2 inhibitors on the mass of skeletal muscle using several mouse models. Treatment with empagliflozin improved the reduction of skeletal muscle mass in Akita mice, which developed diabetes due to pancreatic β cell dysfunction [38]. Also treatment with CANA recovered the reduction of skeletal muscle mass in high-fat diet (HFD)-fed mice, accompanied by increased food intake [39]. As our findings showed that the administration of CANA decreases the skeletal muscle mass during the pair-feeding, but not during the *ad libitum* feeding, further studies will be needed to ask whether SGLT2 inhibitors can affect the skeletal muscle mass in various conditions, including diabetes or HFD-fed state under food restriction.

There is considerable evidence that fast muscle produces ATP mostly via glycolysis, whereas slow muscle does so via the TCA cycle more efficiently [3]. Negative energy balance and reduced blood insulin level during SGLT2 inhibition should induce a variety of catabolic responses outside the skeletal muscles, such as adipose tissue lipolysis, which could contribute to the increased production of FFA and ketone bodies [40]. Evidence has suggested that chronic hyperketonemia in response to SGLT2 inhibition could produce efficient energy via oxidation as a fuel for peripheral tissues, including the skeletal muscle [41]. In this study, ATP production in

fast muscle is slightly increased in CANA-treated mice, during the *ad libitum* feeding, but is reduced during the pair-feeding. There is no significant reduction of ATP production in slow muscle from CANA-treated mice even during the pair-feeding. It is, therefore, conceivable that slow muscle is capable of using more substrates such as FFA and β-OHB, and amino acids than fast muscle, to maintain ATP production. In this setting, fast muscle function is increased, but slow muscle function is unaffected in CANA-treated mice, when fed *ad libitum*. However, fast muscle function is reduced in CANA-treated mice during the pair-feeding, when slow muscle function is unaffected. It is likely that CANA maintains ATP production and metabolites from FFA and amino acids (Supplementary Figure S10A), thus maintaining slow muscle function even during the pair-feeding, when glycolytic flux is reduced in fast muscle as a result of reduced glucose supply, thus reducing fast muscle function (Supplementary Figure S10B). Further studies with low carbohydrate or even ketogenic diets are required to elucidate how much glucose is critical in the regulation of slow and fast muscle function during SGLT2 inhibition.

In this study, CANA tended to increase AMPK phosphorylation in fast muscle preferentially over slow muscle, although there is no significant difference. In addition, CANA significantly decreased mTOR phosphorylation in fast muscle, but not in slow muscle. It is likely that the decreased mTOR phosphorylation in fast muscles, but not in slow muscles, led to reduce fast muscle mass in CANA-treated mice during the 4-week pair-feeding. These differential effects of CANA on the phosphorylation of AMPK and mTOR between slow and fast muscle suggest one of the underlying mechanisms by which CANA affects slow and fast muscle mass and function differentially that we observe. Taken together, it is not likely that CANA has a direct effect on muscles, but it is conceivable that CANA affects metabolic pathways in remote organs such as the muscles, by promoting urinary glucose excretion.

The phosphorylation site of Ser^{2448} on mTOR is associated with activation [42] and is phosphorylated in response to Akt activation [43,44]. In subsequent studies, Akt directly phosphorylates TSC1/2 and inhibits its function, subsequently leading to the activation of mTOR [45,46]. In our study, CANA did not affect Akt phosphorylation, whereas CANA reduced Ser^{2448} phosphorylation on mTOR in fast muscle in the fasting state. Considering that AMPK phosphorylates and activates TSC2, thereby inhibiting mTOR activation in response to changes in the intracellular AMP/ATP ratio [47], it is possible that CANA reduced mTOR phosphorylation by slightly increased AMPK phosphorylation, accompanied with elevated AMP/ATP ratio in fast muscle. Since feeding state can affect the phosphorylation of Akt, AMPK, and mTOR, further study will be needed to investigate how CANA affects mTOR phosphorylation in several feeding states.

Regarding the effect of SGLT2 inhibitors on AMPK phosphorylation, there have been some reports on the difference for AMPK phosphorylation among CANA, dapagliflozin, and empagliflozin. It is reported that CANA can increase p-AMPK expression in HEK-293 cells, whereas dapagliflozin and empagliflozin can increase p-AMPK expression with high concentrations [27]. However, oral administration of CANA in mice increased AMPK phosphorylation in liver, but not affected in muscle [27], which is in part consistent with our study. Currently, there have been some reports that not only CANA but also other SGLT2 inhibitors increase AMPK phosphorylation [48]; dapagliflozin increased AMPK phosphorylation in myofibroblasts and in high glucose-treated HK-2 cells [49,50], while empagliflozin increased AMPK phosphorylation in myocardial infarction hearts [51] and improved hepatic steatosis by increasing AMPK phosphorylation [52]. Therefore, SGLT2 inhibitors could increase AMPK phosphorylation by different concentrations in various cells or tissues, although not significantly observed in the skeletal muscles from nondiabetic mice in this study. Taken together, it is conceivable that SGLT2 inhibitors have a class effect on the AMPK phosphorylation. However, there have been few reports on the differential effect of SGLT2 inhibitors, such as dapagliflozin and empagliflozin, on the slow and fast muscle metabolism, including metabolome analysis. Therefore, further study will be needed to ask whether SGLT2 inhibitors have a class effect on exactly the same findings such as muscle metabolism, mass, and function.

The activity of the IGF-1/PI3K/Akt pathway and its downstream targets plays a critical role in the regulation of skeletal muscle mass [53–55]. Evidence suggested that SGLT2 inhibitors improve the skeletal muscle insulin sensitivity [56,57]. In this study, we also found increased insulin-stimulated p-Akt in slow muscle more than in fast muscle from CANA-treated mice during the pair-feeding experiment. This is consistent with a previous report that slow muscle has greater insulin binding capacity, insulin receptor kinase activity, and autophosphorylation relative to fast muscle [58]. Although HOMA-IR was not different among the groups, it is conceivable that CANA can increase insulin sensitivity in the muscles, but without affecting systemic insulin sensitivity in

Biochemical Journal (2022) 479 425–444
https://doi.org/10.1042/BCJ20210700

nondiabetic mice. The difference in insulin signaling between slow and fast muscles may result in their differential responses to SGLT2 inhibition.

There are limitations in the current study. (1) We used nondiabetic C57BL/6J mice, which enabled us to assess the effect of SGLT2 inhibition on skeletal muscle independently of impaired glucose metabolism. Considering that diabetes is often associated with increased risk of sarcopenia, leading to physical inactivity, and metabolic disorders especially in older patients [59], and that diabetes is also known to reduce slow muscle mass and function compared with fast muscle [60], further studies with diabetic mice of various etiologies are required to elucidate the differential effect of SGLT2 inhibition on slow and fast muscles in impaired glucose metabolism. (2) We used only male mice. Accumulating evidence has suggested that estrogen plays an important role in the muscle function [61]. Importantly, loss of estrogenic function contributes to alter muscle function and increases the risk of various chronic diseases including sarcopenia, type 2 diabetes, metabolic syndrome, and cardiovascular disease [62]. To exclude the direct effect of estrogen on muscle function, only male mice were used in this study. (3) Metabolome analysis during the 2-week *ad libitum* feeding was obtained from two replicates. Therefore, increased number of samples in metabolome analysis will be needed for better understanding of this study. (4) We measured several gene expressions including ATGL, HSL, and GLUT4, but enzyme activities are not measured for the understanding of the mechanism, indicating the limitation for the interpretation of this study.

In conclusion, this study demonstrates the differential effect of SGLT2 inhibition on slow and fast muscles, which is affected by the amount of food intake. The fiber type-specific effect of SGLT2 inhibition might be explained by the fiber type-specific metabolic properties; during SGLT2 inhibition, fast muscle, where glycolytic metabolites are used to produce ATP, is more affected as a result of selective loss of glucose, than slow muscle, where substrates besides glucose, such as FFA and amino acids, can be used to produce ATP via fatty acid β-oxidation. The data of this study provide insights into how SGLT2 inhibitors should be used for the treatment of patients with diabetes, who are at a high risk of sarcopenia.

Materials and methods

Animals and experimental protocols

Eleven-week-old C57BL/6J male mice were purchased from Charles River Laboratories Japan Inc. (Yokohama, Japan). The animals were housed in a temperature-, humidity-, and light-controlled room (12-h light and 12-h dark cycle) and allowed free access to water and normal chow diet (ORIENTAL YEAST CO., LTD. Tokyo, Japan) at Research Center for Human Disease Modeling, Graduate School of Medical Sciences, Kyushu University (Fukuoka, Japan). The animal room was kept at 23 °C during the experiments. CANA was provided by Mitsubishi Tanabe Pharma Corporation, Medicinal Chemistry Laboratory (Saitama, Japan). Twelve-week-old C57BL/6J male mice were fed *ad libitum* with or without 0.03% (w/w) CANA for 2 or 4 weeks. The dose of CANA was set at 30 mg/kg, equivalent to 0.03% (w/w), which has been shown to be an effective pharmacological dose in C57BL/6J mice [63]. The duration of CANA treatment for mice were determined based on the previous study where 4-week administration of 30 mg/kg CANA reduced BW and BG levels in C57BL/6J mice [64]. Food intake was monitored for 3 consecutive days at each week by weighing the mouse feeder MF-4S (SHIN FACTORY, Fukuoka, Japan), and the average daily food intake was calculated. In the pair-feeding experiment, 12-week-old mice were fed with 3.0 g/day of normal chow diet with or without 0.03% (w/w) CANA for 2 or 4 weeks. BW and random BG were monitored once a week during the experiments.

At the end of the experiments, mice were anesthetized with isopentane, and blood samples were obtained from the inferior vein. The weight of the muscles, liver, and eWAT was measured. The slice through the entire midbelly of SOL, EDL, and tibialis anterior (TA) was mounted on cork in optimal cutting temperature, compounded, and frozen in cooled liquid isopentane. Samples were stored at −80°C until use. SOL was examined as slow muscle, while EDL and TA were examined as fast muscles. All experimental protocols were reviewed and approved by the Committee on the Ethics of Animal Experiments, Kyushu University (Protocol #A19-117-4). All methods involving animals were performed in accordance with the relevant guidelines and regulations.

Assays for biochemical parameters

BG levels were measured using the Stat Strip XP3 (NIPRO, Osaka, Japan), which is a glucose oxidase-based glucose meter. Serum insulin concentrations were measured using enzyme-linked immunosorbent assays

(ELISA) (Morinaga Institute of Biological Science, Yokohama, Japan). Blood β-hydroxybutyric acid (β-OHB) was measured using an automatic ketometer (Nipro, Osaka, Japan).

Grip strength measurement and treadmill exercise

Grip strength of mice was measured with MK-380CM/R (Muromachi Kikai, Tokyo, Japan). After the forelimbs and hindlimbs were placed on a mesh, mice were gently pulled back until it lost its grip from the mesh. The maximal force generated at the point where the animal loses its grip was measured. The highest score among five trials with 30-s recovery period was recorded.

Treadmill exercise test was performed as previously described [65] using Ratbelt-2000 (ARCO SYSTEM, Chiba, Japan). All mice were acclimated 4–5 days prior to the exercise test session. After acclimation, they were allowed to rest for at least 2 days. The exercise test session began at a rate of 12 m/min for 40 min, and thereafter, the speed was increased at the rate of 1 m/min every 10 min for a total of 30 min, and then increased at the rate of 1 m/min every 5 min until they were exhausted (mice spent more than 5 s on the electric shocker without resuming running). The running time was measured and the running distance was calculated.

Quantitative real-time PCR analysis

Total RNA was extracted from the muscle and cDNA was synthesized as described previously [66]. The PCR primers used are listed in Supplementary Table S1. mRNA levels were normalized to those of 18S mRNA.

Determination of mitochondrial content

Sections from the muscles were stained for SDH (complex II of the respiratory chain), reflecting oxidative metabolism as previously described [67]. Sections were captured on BZ-8000 microscope (Keyence, Osaka, Japan). For mitochondrial content determination, the mean gray intensity for sections were measured using BZ-II Analyzer (Keyence), allowing the evaluation of mitochondrial content.

Determination of fiber type

The sections of each muscle were immunolabeled for different MyHC as previously described [68]. Briefly, the cross-sections were used to be immunolabeled for MyHC type I, IIa, and IIb. They were allowed to reach room temperature and rehydrated with PBS (pH 7.2). These sections were then blocked by goat serum (10% in PBS) and incubated for 1 h at room temperature with the primary antibody cocktail. The muscle cross-sections were then washed three times in PBS before incubation for 1 h at room temperature with the secondary antibody cocktail. Cross-sections were then washed three times in PBS and slides were cover-slipped by VECTASHIELD Hard Set Mounting Medium (Vector Laboratories, H-1400). All primary antibodies for MyHC were purchased from the Developmental Studies Hybridoma Bank (DSHB, University of Iowa, IA). Antibodies used are listed in Supplementary Table S2.

Western blotting

Fresh mouse muscles were homogenized in the RIPA buffer containing protein inhibitor (Nacalai tesque, Kyoto, Japan) and a phosphatase inhibitor (PhosSTOP, Roche, Switzerland), prior to SDS–PAGE. Protein bands were visualized using the ECL Western Blotting Detection System (GE Healthcare, Buckinghamshire, U. K.) and bands densities were assessed by Image J (NIH). The phosphorylation of AMPK (p-AMPK), mTOR (p-mTOR), and Akt (p-Akt) was evaluated by collecting SOL and EDL after 6 h of fasting. In addition, Akt phosphorylation by insulin stimulation was evaluated by administering 0.5 U/kg of insulin from the inferior vena cava and collecting SOL and EDL 10 min later. Antibodies used are listed in Supplementary Table S3.

Metabolome analysis

Metabolite extraction was performed from the crushed frozen skeletal muscle using the Bligh and Dyer's method with minor modifications [69]. Samples were mixed with 1 ml of solvent mixture ($MeOH : CHCl_3 : H_2O = 10 : 4 : 4$ v/v/v) containing phosphatidylcholine (PC) 15 : 0–18 : 1 (d_7) (2.1 μM), phosphatidylethanolamine (PE) 15 : 0–18 : 1 (d_7) (0.07 μM), phosphatidylserine (PS) 15 : 0–18 : 1 (d_7) (0.064 μM), phosphatidylglycerol (PG) 15 : 0–18 : 1 (d_7) (0.39 μM), phosphatidylinositol (PI) 15 : 0–18 : 1 (d_7) (0.12 μM), phosphatidic acid (PA) 15 : 0–18 : 1 (d_7) (0.10 μM), lysophosphatidylcholine (LPC)18 : 1 (d_7) (0.47 μM), lysophosphatidylethanolamine (LPE) 18 : 1 (d_7) (0.10 μM), cholesteryl ester (CE) 18 : 1 (d_7) (5.3 μM), monoacylglycerol (MG) 18 : 1 (d_7) (0.055 μM), diacylglycerol (DG) 15 : 0–18 : 1 (d_7) (0.17 μM), triacylglycerol (TG) 15 : 0–18 : 1 (d_7)

Biochemical Journal (2022) 479 425–444
https://doi.org/10.1042/BCJ20210700

(0.68 μM), sphingomyelin (SM) d18 : 1–18 : 1 (d_9) (0.41 μM), cholesterol (d_7) (2.5 μM), ceramide (Cer) d18 : 1–17 : 0 (0.50 μM), hexosylceramide (HexCer) d18 : 1–12 : 0 (0.50 μM), FFA 17 : 0 (0.50 μM), and piperazine-1,4-bis(2-ethanesulfonic acid) (PIPES) (0.63 μM) as internal standards for mass spectrometry-based metabolome analysis. These tubes were vortexed for 60 s, which were subjected to ultrasonic waves for extraction and centrifuged (16 000 × g, 4 °C, 5 min) to remove impurities and foreign substances. Then, 700 μL of the supernatant was transferred to 2 ml Eppendorf tube. After adding 155 μL of H_2O and 235 μL of $CHCl_3$, phase separation of aqueous and organic layers was performed by centrifugation (16 000×**g**, 4°C, 3 min). The aqueous (upper) layer (400 μL) was transferred to a clean tube for analysis by an ion chromatography with a Dionex IonPac AS11-HC-4 μm column (2 mm i.d. 250 mm, 4 μm particle size, Thermo Fisher Scientific, Waltham, MA, U.S.A.) coupled with a quadrupole-Orbitrap mass spectrometry (IC/MS) (Thermo Fisher Scientific) for anionic polar metabolites (i.e. organic acids, nucleotides, etc.) [70,71] and a liquid chromatography with a Discovery HS F5 column (2.1 mm i.d. 150 mm, 3 μm particle size, Merck, Darmstadt, Germany) coupled with a quadrupole-Orbitrap mass spectrometry (PFPP-LC/MS) (Thermo Fisher Scientific) for cationic polar metabolites (i.e. amino acids, etc.) [70,71]. After the aqueous layer extracts were evaporated under vacuum, dried extracts were stored at −80°C until use for IC/MS and PFPP-LC/MS analysis. The organic (lower) layer (200 μL) obtained by phase separation. Finally, 400 μL of MeOH was added and stored at −80°C until analysis. The levels of each hydrophobic metabolites (i.e. TG and CE) were quantified using supercritical fluid chromatography with an ACQUITY UPC^2 HSS C18 column (3.0 mm i.d. 100 mm, 1.8 μm particle size, Waters, Milford, MA) coupled with a triple quadrupole mass spectrometry (C18-SFC/MS/MS) in multiple reactions monitoring (MRM) mode; the SFC/MS/MS system comprised a SFC (Nexera UC; Shimadzu, Kyoto, Japan) and a triple quadrupole mass spectrometer (LCMS-8060; Shimadzu) [72]. The levels of other lipids (i.e. PC, PE, PS, PG, PI, PA, LPC, LPE, MG, DG, SM, cholesterol, Cer, HexCer, and FFA) were quantified using SFC with an ACQUITY UPC2 Torus diethylamine (DEA) (3.0 mm i.d. 100 mm, 1.8 μm particle size, Waters) coupled with a triple quadrupole mass spectrometry (DEA-SFC/MS/MS) in MRM mode [73]. Supplementary Tables S4–S9 list the abbreviations of the hydrophilic and hydrophobic metabolites.

DNA microarray analysis

According to the manufacturer's instructions, the cRNA was amplified and labeled using Low Input Quick Amp Labeling, and hybridized using SurePrint G3 Mouse Gene Expression Microarray 8 × 60 K v2 (Agilent Technologies, Santa Clara, CA, U.S.A.). All hybridized microarray slides were scanned using an Agilent scanner. Relative hybridization intensities and background hybridization values were calculated using Agilent Feature Extraction Software (ver. 9.5.1.1).

Statistical Analysis

All data were expressed as the means ± SEM. Statistical analysis was performed with Student's *t*-test or one-way ANOVA with Fisher's protected least significant difference test. $P < 0.05$ was considered statistically significant.

Data Availability

Full data will be provided upon reasonable request.

Competing Interests

Y.O. has received research grants from Mitsubishi Tanabe Pharma Corporation. No other potential conflicts of interest relevant to this article were reported.

Funding

This study was supported in part by Grants-in-Aid for Scientific Research from a Japan Society for the Promotion of Science (JSPS) (21K16371 to H.Y. and 19H01054 to Y.O.), AMED-CREST Program (18gm0610011h9905 to Y.O.), and Mitsui Sumitomo Insurance Welfare Foundation (to H.Y.), and research grants from Mitsubishi Tanabe Pharma Cooperation. This study was also supported in part by the AMED-CREST (21gm0910010h0206, 21gm0910013h0005, and 21gm1010010s0204) (Y.I., T.B.), a grant from the JST-CREST Program (JPMJCR15G4) (T.B.), JST-Mirai Program Common Platform Technology (Y.I.), JSPS Grant-in-Aid for Scientific Research on Innovative Areas 17H06304 (T.B.), and the Cooperative Research Project Program of the Medical Institute of Bioregulation, Kyushu University.

PORTLAND PRESS

CRediT Author Contribution

Hisashi Yokomizo: Conceptualization, data curation, formal analysis, supervision, funding acquisition, validation, investigation, methodology, writing—original draft, project administration, writing—review and editing. **Hiroko Otsuka**: Conceptualization, data curation, formal analysis, supervision, validation, investigation, methodology, writing—original draft, project administration, writing—review and editing. **Shintaro Nakamura**: Data curation, formal analysis, validation, investigation, methodology. **Yoshihiro Izumi**: Data curation, formal analysis, supervision, funding acquisition, validation, methodology, writing— review and editing. **Masatomo Takahashi**: Data curation, formal analysis, supervision, validation, methodology. **Sachiko Obara**: Data curation, formal analysis, validation, methodology. **Motonao Nakao**: Data curation, formal analysis, validation, methodology. **Yosuke Ikeda**: Data curation, formal analysis, validation, investigation, methodology. **Naoichi Sato**: Data curation, formal analysis, validation, investigation, methodology, writing—review and editing. **Ryuichi Sakamoto**: data curation, formal analysis, validation, investigation, methodology, project administration, writing—review and editing. **Yasutaka Miyachi**: Data curation, formal analysis, validation, investigation, methodology, writing—review and editing. **Takashi Miyazawa**: Conceptualization, data curation, formal analysis, supervision, validation, investigation, methodology, project administration, writing—review and editing. **Takeshi Bamba**: Conceptualization, resources, data curation, formal analysis, supervision, funding acquisition, validation, investigation, methodology, project administration, writing—review and editing. **Yoshihiro Ogawa**: Conceptualization, resources, data curation, software, formal analysis, supervision, funding acquisition, validation, investigation, methodology, writing—original draft, project administration, writing—review and editing.

Acknowledgements

The authors thank all the members from the Ogawa laboratory for discussion. We would like to thank Kaori Yasuda (Cell Innovator, Inc.) for the technical support. We are also grateful to Dr. Noriyuki Sonoda for encouragement.

Abbreviations

ACO, acyl-CoA oxidase; ALT, alanine aminotransferase; ATGL, adipose triglyceride lipase; CANA, canagliflozin; EDL, extensor digitorum longus; eWAT, epididymal white adipose tissue; F6P, fructose 6-phosphate; Fast muscle, fast skeletal muscle; FBP, fructose 1,6-bisphosphate; FFA, free fatty acids; FoxO1, forkhead box transcription factor O1; G6P, glucose-6-phosphate; GS, glutamine synthetase; HK2, hexokinase 2; HOMA-IR, homeostasis model assessment of insulin resistance; HSL, hormone-sensitive lipase; LAT2, L-type amino acid transporter 2; LC3B, microtubule-associated protein 1 light chain 3 β; MCAD, acetyl-CoA dehydrogenase, medium chain; MuRF1, muscle RING-finger protein-1; MyHC, myosin heavy chain; NASH, nonalcoholic steatohepatitis; PDHA1, pyruvate dehydrogenase E1 subunit α 1; PEP, phosphoenolpyruvic acid; PFKm, phosphofructokinase, muscle; PGC1α, peroxisome proliferator-activated receptor α co-activator 1α; PI3K, phosphatidylinositol 3'-kinase; PKm1, pyruvate kinase muscle isozyme 1; PPARA, peroxisome proliferator-activated receptor α; SDH, succinate dehydrogenase; SGLT2, sodium–glucose cotransporter 2; SOL, soleus; slow muscle, slow skeletal muscle; TA, tibialis anterior; β-OHB, β-hydroxybutyric acid.

References

1 Petersen, K.F., Dufour, S., Savage, D.B., Bilz, S., Solomon, G., Yonemitsu, S. et al. (2007) The role of skeletal muscle insulin resistance in the pathogenesis of the metabolic syndrome. *Proc. Natl Acad. Sci. U.S.A.* **104**, 12587–12594 https://doi.org/10.1073/pnas.0705408104

2 Wu, H. and Ballantyne, C.M. (2017) Skeletal muscle inflammation and insulin resistance in obesity. *J. Clin. Invest.* **127**, 43–54 https://doi.org/10.1172/JCI88880

3 Schiaffino, S. and Reggiani, C. (2011) Fiber types in mammalian skeletal muscles. *Physiol. Rev.* **91**, 1447–1531 https://doi.org/10.1152/physrev.00031.2010

4 Picard, M., Hepple, R.T. and Burelle, Y. (2012) Mitochondrial functional specialization in glycolytic and oxidative muscle fibers: tailoring the organelle for optimal function. *Am. J. Physiol. Cell Physiol.* **302**, C629–C641 https://doi.org/10.1152/ajpcell.00368.2011

5 Smerdu, V., Karsch-Mizrachi, I., Campione, M., Leinwand, L. and Schiaffino, S. (1994) Type IIx myosin heavy chain transcripts are expressed in type IIb fibers of human skeletal muscle. *Am. J. Physiol.* **267**, C1723–C1728 https://doi.org/10.1152/ajpcell.1994.267.6.C1723

6 Blaauw, B., Schiaffino, S. and Reggiani, C. (2013) Mechanisms modulating skeletal muscle phenotype. *Comp. Physiol.* **3**, 1645–1687 https://doi.org/10.1002/cphy.c130009

7 Mackrell, J.G. and Cartee, G.D. (2012) A novel method to measure glucose uptake and myosin heavy chain isoform expression of single fibers from rat skeletal muscle. *Diabetes* **61**, 995–1003 https://doi.org/10.2337/db11-1299

8 Albers, P.H., Pedersen, A.J., Birk, J.B., Kristensen, D.E., Vind, B.F., Baba, O. et al. (2015) Human muscle fiber type-specific insulin signaling: impact of obesity and type 2 diabetes. *Diabetes* **64**, 485–497 https://doi.org/10.2337/db14-0590

Biochemical Journal (2022) **479** 425–444
https://doi.org/10.1042/BCJ20210700

9 Stuart, C.A., McCurry, M.P., Marino, A., South, M.A., Howell, M.E., Layne, A.S. et al. (2013) Slow-twitch fiber proportion in skeletal muscle correlates with insulin responsiveness. *J. Clin. Endocrinol. Metab.* **98**, 2027–2036 https://doi.org/10.1210/jc.2012-3876

10 Marin, P., Andersson, B., Krotkiewski, M. and Bjorntorp, P. (1994) Muscle fiber composition and capillary density in women and men with NIDDM. *Diabetes Care* **17**, 382–386 https://doi.org/10.2337/diacare.17.5.382

11 Wang, Y. and Pessin, J.E. (2013) Mechanisms for fiber-type specificity of skeletal muscle atrophy. *Curr. Opin. Clin. Nutr. Metab. Care* **16**, 243–250 https://doi.org/10.1097/MCO.0b013e328360272d

12 Landi, F., Onder, G. and Bernabei, R. (2013) Sarcopenia and diabetes: two sides of the same coin. *J. Am. Med. Dir. Assoc.* **14**, 540–541 https://doi.org/10.1016/j.jamda.2013.05.004

13 Ciciliot, S., Rossi, A.C., Dyar, K.A., Blaauw, B. and Schiaffino, S. (2013) Muscle type and fiber type specificity in muscle wasting. *Int. J. Biochem. Cell Biol.* **45**, 2191–2199 https://doi.org/10.1016/j.biocel.2013.05.016

14 Bolinder, J., Ljunggren, O., Johansson, L., Wilding, J., Langkilde, A.M., Sjostrom, C.D. et al. (2014) Dapagliflozin maintains glycaemic control while reducing weight and body fat mass over 2 years in patients with type 2 diabetes mellitus inadequately controlled on metformin. *Diabetes Obes. Metab.* **16**, 159–169 https://doi.org/10.1111/dom.12189

15 Zaccardi, F., Webb, D.R., Htike, Z.Z., Youssef, D., Khunti, K. and Davies, M.J. (2016) Efficacy and safety of sodium–glucose co-transporter-2 inhibitors in type 2 diabetes mellitus: systematic review and network meta-analysis. *Diabetes Obes. Metab.* **18**, 783–794 https://doi.org/10.1111/dom.12670

16 Komiya, C., Tsuchiya, K., Shiba, K., Miyachi, Y., Furuke, S., Shimazu, N. et al. (2016) Ipragliflozin improves hepatic steatosis in obese mice and liver dysfunction in type 2 diabetic patients irrespective of body weight reduction. *PLoS One* **11**, e0151511 https://doi.org/10.1371/journal.pone.0151511

17 Shiba, K., Tsuchiya, K., Komiya, C., Miyachi, Y., Mori, K., Shimazu, N. et al. (2018) Canagliflozin, an SGLT2 inhibitor, attenuates the development of hepatocellular carcinoma in a mouse model of human NASH. *Sci Rep.* **8**, 2362 https://doi.org/10.1038/s41598-018-19658-7

18 Zinman, B., Wanner, C., Lachin, J.M., Fitchett, D., Bluhmki, E., Hantel, S. et al. (2015) Empagliflozin, cardiovascular outcomes, and mortality in type 2 diabetes. *N. Engl. J. Med.* **373**, 2117–2128 https://doi.org/10.1056/NEJMoa1504720

19 Perkovic, V., Jardine, M.J., Neal, B., Bompoint, S., Heerspink, H.J.L., Charytan, D.M. et al. (2019) Canagliflozin and renal outcomes in type 2 diabetes and nephropathy. *N. Engl. J. Med.* **380**, 2295–2306 https://doi.org/10.1056/NEJMoa1811744

20 Sugiyama, S., Jinnouchi, H., Kurinami, N., Hieshima, K., Yoshida, A., Jinnouchi, K. et al. (2018) Dapagliflozin reduces fat mass without affecting muscle mass in type 2 diabetes. *J. Atheroscler. Thromb.* **25**, 467–476 https://doi.org/10.5551/jat.40873

21 Sasaki, T., Sugawara, M. and Fukuda, M. (2019) Sodium–glucose cotransporter 2 inhibitor-induced changes in body composition and simultaneous changes in metabolic profile: 52-week prospective LIGHT (luseogliflozin: the components of weight loss in Japanese patients with type 2 diabetes mellitus) study. *J. Diabetes Investig.* **10**, 108–117 https://doi.org/10.1111/jdi.12851

22 Bouchi, R., Terashima, M., Sasahara, Y., Asakawa, M., Fukuda, T., Takeuchi, T. et al. (2017) Luseogliflozin reduces epicardial fat accumulation in patients with type 2 diabetes: a pilot study. *Cardiovasc. Diabetol.* **16**, 32 https://doi.org/10.1186/s12933-017-0516-8

23 Obata, A., Kubota, N., Kubota, T., Iwamoto, M., Sato, H., Sakurai, Y. et al. (2016) Tofogliflozin improves insulin resistance in skeletal muscle and accelerates lipolysis in adipose tissue in male mice. *Endocrinology* **157**, 1029–1042 https://doi.org/10.1210/en.2015-1588

24 Packer, M., Anker, S.D., Butler, J., Filippatos, G., Pocock, S.J., Carson, P. et al. (2020) Cardiovascular and renal outcomes with empagliflozin in heart failure. *N. Engl. J. Med.* **383**, 1413–1424 https://doi.org/10.1056/NEJMoa2022190

25 McMurray, J.J.V., Solomon, S.D., Inzucchi, S.E., Kober, L., Kosiborod, M.N., Martinez, F.A. et al. (2019) Dapagliflozin in patients with heart failure and reduced ejection fraction. *N. Engl. J. Med.* **381**, 1995–2008 https://doi.org/10.1056/NEJMoa1911303

26 Heerspink, H.J.L., Stefansson, B.V., Correa-Rotter, R., Chertow, G.M., Greene, T., Hou, F.F. et al. (2020) Dapagliflozin in patients with chronic kidney disease. *N. Engl. J. Med.* **383**, 1436–1446 https://doi.org/10.1056/NEJMoa2024816

27 Hawley, S.A., Ford, R.J., Smith, B.K., Gowans, G.J., Mancini, S.J., Pitt, R.D. et al. (2016) The Na+/glucose cotransporter inhibitor canagliflozin activates AMPK by inhibiting mitochondrial function and increasing cellular AMP levels. *Diabetes* **65**, 2784–2794 https://doi.org/10.2337/db16-0058

28 Kalyani, R.R., Corriere, M. and Ferrucci, L. (2014) Age-related and disease-related muscle loss: the effect of diabetes, obesity, and other diseases. *Lancet Diabetes Endocrinol.* **2**, 819–829 https://doi.org/10.1016/S2213-8587(14)70034-8

29 O'Neill, B.T., Lee, K.Y., Klaus, K., Softic, S., Krumpoch, M.T., Fentz, J. et al. (2016) Insulin and IGF-1 receptors regulate FoxO-mediated signaling in muscle proteostasis. *J. Clin. Invest.* **126**, 3433–3446 https://doi.org/10.1172/JCI86522

30 Bolinder, J., Ljunggren, O., Kullberg, J., Johansson, L., Wilding, J., Langkilde, A.M. et al. (2012) Effects of dapagliflozin on body weight, total fat mass, and regional adipose tissue distribution in patients with type 2 diabetes mellitus with inadequate glycemic control on metformin. *J. Clin. Endocrinol. Metab.* **97**, 1020–1031 https://doi.org/10.1210/jc.2011-2260

31 Marton, A., Kaneko, T., Kovalik, J.P., Yasui, A., Nishiyama, A., Kitada, K. et al. (2021) Organ protection by SGLT2 inhibitors: role of metabolic energy and water conservation. *Nat. Rev. Nephrol.* **17**, 65–77 https://doi.org/10.1038/s41581-020-00350-x

32 Sano, M., Meguro, S., Kawai, T. and Suzuki, Y. (2016) Increased grip strength with sodium–glucose cotransporter 2. *J. Diabetes* **8**, 736–737 https://doi.org/10.1111/1753-0407.12402

33 Avruch, J., Lin, Y., Long, X., Murthy, S. and Ortiz-Vega, S. (2005) Recent advances in the regulation of the TOR pathway by insulin and nutrients. *Curr. Opin. Clin. Nutr. Metab. Care* **8**, 67–72 https://doi.org/10.1097/00075197-200501000-00010

34 Zhao, J., Brault, J.J., Schild, A., Cao, P., Sandri, M., Schiaffino, S. et al. (2007) Foxo3 coordinately activates protein degradation by the autophagic/lysosomal and proteasomal pathways in atrophying muscle cells. *Cell Metab.* **6**, 472–483 https://doi.org/10.1016/j.cmet.2007.11.004

35 Sanchez, A.M., Candau, R.B. and Bernardi, H. (2014) Foxo transcription factors: their roles in the maintenance of skeletal muscle homeostasis. *Cell Mol. Life Sci.* **71**, 1657–1671 https://doi.org/10.1007/s00018-013-1513-z

36 Mammucari, C., Milan, G., Romanello, V., Masiero, E., Rudolf, R., Del Piccolo, P. et al. (2007) $Foxo_3$ controls autophagy in skeletal muscle in vivo. *Cell Metab.* **6**, 458–471 https://doi.org/10.1016/j.cmet.2007.11.001

37 Goodman, C.A., Kotecki, J.A., Jacobs, B.L. and Hornberger, T.A. (2012) Muscle fiber type-dependent differences in the regulation of protein synthesis. *PLoS One* **7**, e37890 https://doi.org/10.1371/journal.pone.0037890

38 Hirata, Y., Nomura, K., Senga, Y., Okada, Y., Kobayashi, K., Okamoto, S. et al. (2019) Hyperglycemia induces skeletal muscle atrophy via a WWP1/KLF15 axis. *JCI Insight* **4**, e124952 https://doi.org/10.1172/jci.insight.124952

39 Naznin, F., Sakoda, H., Okada, T., Tsubouchi, H., Waise, T.M., Arakawa, K. et al. (2017) Canagliflozin, a sodium glucose cotransporter 2 inhibitor, attenuates obesity-induced inflammation in the nodose ganglion, hypothalamus, and skeletal muscle of mice. *Eur. J. Pharmacol.* **794**, 37–44 https://doi.org/10.1016/j.ejphar.2016.11.028
40 Ferrannini, E., Mark, M. and Mayoux, E. (2016) CV protection in the EMPA-REG OUTCOME Trial: a "Thrifty Substrate" hypothesis. *Diabetes Care* **39**, 1108–1114 https://doi.org/10.2337/dc16-0330
41 Qiu, H., Novikov, A. and Vallon, V. (2017) Ketosis and diabetic ketoacidosis in response to SGLT2 inhibitors: basic mechanisms and therapeutic perspectives. *Diabetes Metab. Res. Rev.* **33**, e2886 https://doi.org/10.1002/dmrr.2886
42 Bolster, D.R., Crozier, S.J., Kimball, S.R. and Jefferson, L.S. (2002) AMP-activated protein kinase suppresses protein synthesis in rat skeletal muscle through down-regulated mammalian target of rapamycin (mTOR) signaling. *J. Biol. Chem.* **277**, 23977–23980 https://doi.org/10.1074/jbc.C200171200
43 Sekulic, A., Hudson, C.C., Homme, J.L., Yin, P., Otterness, D.M., Karnitz, L.M. et al. (2000) A direct linkage between the phosphoinositide 3-kinase-AKT signaling pathway and the mammalian target of rapamycin in mitogen-stimulated and transformed cells. *Cancer Res.* **60**, 3504–3513 PMID: 10910062
44 Reynolds, T.H.T., Bodine, S.C. and Lawrence, Jr, J.C. (2002) Control of Ser2448 phosphorylation in the mammalian target of rapamycin by insulin and skeletal muscle load. *J. Biol. Chem.* **277**, 17657–17662 https://doi.org/10.1074/jbc.M201142200
45 Garami, A., Zwartkruis, F.J., Nobukuni, T., Joaquin, M., Roccio, M., Stocker, H. et al. (2003) Insulin activation of Rheb, a mediator of mTOR/S6K/4E-BP signaling, is inhibited by TSC1 and 2. *Mol. Cell* **11**, 1457–1466 https://doi.org/10.1016/s1097-2765(03)00220-x
46 Inoki, K., Corradetti, M.N. and Guan, K.L. (2005) Dysregulation of the TSC-mTOR pathway in human disease. *Nat. Genet.* **37**, 19–24 https://doi.org/10.1038/ng1494
47 Inoki, K., Zhu, T. and Guan, K.L. (2003) TSC2 mediates cellular energy response to control cell growth and survival. *Cell* **115**, 577–590 https://doi.org/10.1016/s0092-8674(03)00929-2
48 Uthman, L., Baartscheer, A., Schumacher, C.A., Fiolet, J.W.T., Kuschma, M.C., Hollmann, M.W. et al. (2018) Direct cardiac actions of sodium glucose cotransporter 2 inhibitors target pathogenic mechanisms underlying heart failure in diabetic patients. *Front. Physiol.* **9**, 1575 https://doi.org/10.3389/fphys.2018.01575
49 Ye, Y., Bajaj, M., Yang, H.C., Perez-Polo, J.R. and Birnbaum, Y. (2017) SGLT-2 inhibition with dapagliflozin reduces the activation of the Nlrp3/ASC inflammasome and attenuates the development of diabetic cardiomyopathy in mice with type 2 diabetes. Further augmentation of the effects with Saxagliptin, a DPP4 inhibitor. *Cardiovasc Drugs Ther.* **31**, 119–132 https://doi.org/10.1007/s10557-017-6725-2
50 Xu, J., Kitada, M., Ogura, Y., Liu, H. and Koya, D. (2021) Dapagliflozin restores impaired autophagy and suppresses inflammation in high glucose-treated HK-2 cells. *Cells* **10**, 1457 https://doi.org/10.3390/cells10061457
51 Liu, Y., Wu, M., Xu, J., Xu, B. and Kang, L. (2021) Empagliflozin prevents from early cardiac injury post myocardial infarction in non-diabetic mice. *Eur. J. Pharm. Sci.* **161**, 105788 https://doi.org/10.1016/j.ejps.2021.105788
52 Luo, J., Sun, P., Wang, Y., Chen, Y., Niu, Y., Ding, Y. et al. (2021) Dapagliflozin attenuates steatosis in livers of high-fat diet-induced mice and oleic acid-treated L02 cells via regulating AMPK/mTOR pathway. *Eur. J. Pharmacol.* **907**, 174304 https://doi.org/10.1016/j.ejphar.2021.174304
53 Sandri, M., Sandri, C., Gilbert, A., Skurk, C., Calabria, E., Picard, A. et al. (2004) Foxo transcription factors induce the atrophy-related ubiquitin ligase atrogin-1 and cause skeletal muscle atrophy. *Cell* **117**, 399–412 https://doi.org/10.1016/s0092-8674(04)00400-3
54 Wullschleger, S., Loewith, R. and Hall, M.N. (2006) TOR signaling in growth and metabolism. *Cell* **124**, 471–484 https://doi.org/10.1016/j.cell.2006.01.016
55 James, H.A., O'Neill, B.T. and Nair, K.S. (2017) Insulin regulation of proteostasis and clinical implications. *Cell Metab.* **26**, 310–323 https://doi.org/10.1016/j.cmet.2017.06.010
56 Merovci, A., Solis-Herrera, C., Daniele, G., Eldor, R., Fiorentino, T.V., Tripathy, D. et al. (2014) Dapagliflozin improves muscle insulin sensitivity but enhances endogenous glucose production. *J. Clin. Invest.* **124**, 509–514 https://doi.org/10.1172/JCI70704
57 Ferrannini, E., Muscelli, E., Frascerra, S., Baldi, S., Mari, A., Heise, T. et al. (2014) Metabolic response to sodium–glucose cotransporter 2 inhibition in type 2 diabetic patients. *J. Clin. Invest.* **124**, 499–508 https://doi.org/10.1172/JCI72227
58 Song, X.M., Ryder, J.W., Kawano, Y., Chibalin, A.V., Krook, A. and Zierath, J.R. (1999) Muscle fiber type specificity in insulin signal transduction. *Am. J. Physiol.* **277**, R1690–R1696 https://doi.org/10.1152/ajpregu.1999.277.6.R1690
59 Kim, T.N., Park, M.S., Yang, S.J., Yoo, H.J., Kang, H.J., Song, W. et al. (2010) Prevalence and determinant factors of sarcopenia in patients with type 2 diabetes: the Korean Sarcopenic Obesity Study (KSOS). *Diabetes Care* **33**, 1497–1499 https://doi.org/10.2337/dc09-2310
60 Hickey, M.S., Carey, J.O., Azevedo, J.L., Houmard, J.A., Pories, W.J., Israel, R.G. et al. (1995) Skeletal muscle fiber composition is related to adiposity and in vitro glucose transport rate in humans. *Am. J. Physiol.* **268**, E453–E457 https://doi.org/10.1152/ajpendo.1995.268.3.E453
61 Lowe, D.A. and Kararigas, G. (2020) Editorial: new insights into estrogen/estrogen receptor effects in the cardiac and skeletal muscle. *Front. Endocrinol. (Lausanne)* **11**, 141 https://doi.org/10.3389/fendo.2020.00141
62 Spangenburg, E.E., Geiger, P.C., Leinwand, L.A. and Lowe, D.A. (2012) Regulation of physiological and metabolic function of muscle by female sex steroids. *Med. Sci. Sports Exerc.* **44**, 1653–1662 https://doi.org/10.1249/MSS.0b013e31825871fa
63 Kuriyama, C., Xu, J.Z., Lee, S.P., Qi, J., Kimata, H., Kakimoto, T. et al. (2014) Analysis of the effect of canagliflozin on renal glucose reabsorption and progression of hyperglycemia in zucker diabetic fatty rats. *J. Pharmacol. Exp. Ther.* **351**, 423–431 https://doi.org/10.1124/jpet.114.217992
64 Tanaka, K., Takahashi, H., Katagiri, S., Sasaki, K., Ohsugi, Y., Watanabe, K. et al. (2020) Combined effect of canagliflozin and exercise training on high-fat diet-fed mice. *Am. J. Physiol. Endocrinol. Metab.* **318**, E492–E503 https://doi.org/10.1152/ajpendo.00401.2019
65 Kong, X., Yao, T., Zhou, P., Kazak, L., Tenen, D., Lyubetskaya, A. et al. (2018) Brown adipose tissue controls skeletal muscle function via the secretion of myostatin. *Cell Metab.* **28**, 631–643.e633 https://doi.org/10.1016/j.cmet.2018.07.004
66 Takeichi, Y., Miyazawa, T., Sakamoto, S., Hanada, Y., Wang, L., Gotoh, K. et al. (2021) Non-alcoholic fatty liver disease in mice with hepatocyte-specific deletion of mitochondrial fission factor. *Diabetologia* **64**, 2092–2107 https://doi.org/10.1007/s00125-021-05488-2
67 Gouspillou, G., Sgarioto, N., Norris, B., Barbat-Artigas, S., Aubertin-Leheudre, M., Morais, J.A. et al. (2014) The relationship between muscle fiber type-specific PGC-1alpha content and mitochondrial content varies between rodent models and humans. *PLoS One* **9**, e103044 https://doi.org/10.1371/journal.pone.0103044

Biochemical Journal (2022) **479** 425–444
https://doi.org/10.1042/BCJ20210700

68 Goodman, C.A., Mabrey, D.M., Frey, J.W., Miu, M.H., Schmidt, E.K., Pierre, P. et al. (2011) Novel insights into the regulation of skeletal muscle protein synthesis as revealed by a new nonradioactive in vivo technique. *FASEB J.* **25**, 1028–1039 https://doi.org/10.1096/fj.10-168799

69 Bligh, E.G. and Dyer, W.J. (1959) A rapid method of total lipid extraction and purification. *Can. J. Biochem. Physiol.* **37**, 911–917 https://doi.org/10.1139/o59-099

70 Izumi, Y., Matsuda, F., Hirayama, A., Ikeda, K., Kita, Y., Horie, K. et al. (2019) Inter-laboratory comparison of metabolite measurements for metabolomics data integration. *Metabolites* **9**, 257 https://doi.org/10.3390/metabo9110257

71 Fushimi, T., Izumi, Y., Takahashi, M., Hata, K., Murano, Y. and Bamba, T. (2020) Dynamic metabolome analysis reveals the metabolic fate of medium-chain fatty acids in AML12 cells. *J. Agric. Food Chem.* **68**, 11997–12010 https://doi.org/10.1021/acs.jafc.0c04723

72 Ogawa, T., Izumi, Y., Kusumoto, K., Fukusaki, E. and Bamba, T. (2017) Wide target analysis of acylglycerols in miso (Japanese fermented soybean paste) by supercritical fluid chromatography coupled with triple quadrupole mass spectrometry and the analysis of the correlation between taste and both acylglycerols and free fatty acids. *Rapid Commun. Mass Spectrom.* **31**, 928–936 https://doi.org/10.1002/rcm.7862

73 Takeda, H., Izumi, Y., Takahashi, M., Paxton, T., Tamura, S., Koike, T. et al. (2018) Widely-targeted quantitative lipidomics method by supercritical fluid chromatography triple quadrupole mass spectrometry. *J. Lipid Res.* **59**, 1283–1293 https://doi.org/10.1194/jlr.D083014